Dynamic motions of 1,6-Diphenyl-1,3,5-hexatriene in interdigitated C(18):C(10)phosphatidylcholine bilayers*

Yvonne Lin Kao,[‡] Parkson Lee-Gau Chong,[‡] and Ching-hsien Huang[§]

[‡]Department of Biochemistry, Meharry Medical College, Nashville, Tennessee 37208; and [§]Department of Biochemistry, University of Virginia School of Medicine, Charlottesville, Virginia 22908 USA

ABSTRACT This study investigates the dynamic behavior of 1,6-diphenyl-1,3,5-hexatriene (DPH) in C(18):C(10)phosphatidylcholine [C(18):C(10)PC] bilayers. C(18):C(10)PC is an asymmetric mixed-chain phosphatidylcholine known to form mixed-interdigitated structures below the transition temperature and form partially interdigitated bilayers above the transition temperature. The rotation of DPH in C(18):C(10)PC has been described in terms of the thermal coefficient of rotation using the modified Y-plot method which takes into account the limiting anisotropy value. During the phase transition of C(18):C(10)PC, DPH exhibits a thermal coefficient $b_{2M} = 0.41 - 0.51\ °C^{-1}$ which is similar to the b_{2M} values obtained with noninterdigitated phosphatidylcholine bilayers. Differential polarized phase-modulation fluorometry has also been employed to study the dynamic behavior of DPH in C(18):C(10)PC in real time. The data show that DPH contains considerable motion in the highly ordered mixed interdigitated bilayers. The DPH motion steadily increases with an increase in temperature as shown by the rotational correlation time, and the wobbling diffusion constant. However, the limiting anisotropy, the order parameter, and the width of the lifetime distribution undergo an abrupt decrease, and a corresponding abrupt increase in the cone angle, at ~16°C. This temperature range is near the onset temperature of the phase transition as determined by differential scanning calorimetry. The rotational parameters show strong hysteresis on heating and cooling. All the rotational parameters derived from DPH fluorescence in mixed interdigitated C(18):C(10)PC exhibit magnitudes similar to those obtained from noninterdigitated gel phases of symmetric diacylphosphatidylcholines. These results, combined with those obtained with dehydroergosterol (Kao, Y. L., P. L.-G. Chong, and C. Huang. 1990. *Biochemistry.* 29:1315–1322), suggest that considerable rotational mobility of small molecules can be sustained in an intramolecularly highly ordered interdigitated lipid matrix, implying that the membrane maintains a fluid environment around membrane perturbants even when the lipid matrix is extensively interdigitated.

INTRODUCTION

Research in interdigitated lipid bilayers has been growing rapidly in recent years (reviewed in Huang and Mason, 1986; Slater and Huang, 1988). One of the main interests lies in the dynamic structure of interdigitated lipid membranes. A particular question which needs to be addressed is whether the membrane maintains a fluid dynamic entity when the lipid matrix is extensively interdigitated. According to the fluid mosaic model (Singer and Nicolson, 1972), optimal membrane functions require appropriate membrane fluidity.

Dynamic behavior of the acyl chain in interdigitated structures has been investigated. Raman spectroscopic studies showed a similar intra- and interchain disorder between partially interdigitated lipids and noninterdigitated lipids of the same molecular weight in the liquid-crystalline state (Huang et al., 1982, 1983). In comparison, the hydrocarbon chain of mixed-interdigitated lipid membranes is more ordered than the acyl chain of noninterdigitated lipids of the same molecular weight in the gel state (Huang et al., 1982, 1983). Infrared studies showed that the rotation of the zig-zag plane of the acyl chain in a mixed-interdigitated structure is not completely damped until a pressure of 5.5 kbar is applied (Wong and Huang, 1989). In addition to the acyl chains, the dynamics of the headgroup in interdigitated lipid membranes has also been studied. 1,2-Dihexadecyl-*sn*-glycero-3-phosphocholine (DHPC),[1] for example, is known from x-ray data to form interdigitated structures below 35°C (Ruocco et al., 1985); yet, ^{14}N- and ^{31}P-NMR

*Appendix: A Modified Y-Plot Method by B. Wieb Van Der Meer, Department of Physics and Astronomy, Western Kentucky University, Bowling Green, KY 42101.

Address correspondence to Dr. Chong.

[1]*Abbreviations used in this paper:* C(18):C(10)PC, 1-Stearoyl-2-capryl-*sn*-glycero-3-phosphocholine; DHE, dehydroergosterol; DHPC, 1,2-dihexadecyl-*sn*-glycero-3-phosphocholine; DLPE, 1,2-dilauroyl-*sn*-phosphatidylethanolamine; DMPC, 1,2-dimyristoyl-*sn*-glycerol-3-phosphocholine; DPH, 1,6-diphenyl-1,3,5-hexatriene; DPPC, 1,2-dipalmitoyl-*sn*-glycero-3-phosphocholine; DSC, differential scanning calorimetry; DSPC, 1,2-distearoyl-*sn*-glycero-3-phosphocholine; MLV, multilamellar vesicle; POPOP *p*-bis[2-(5-phenyloxazolyl)]benzene.

0006-3495/90/10/947/10 $2.00

studies (Siminovitch et al., 1983; Ruocco et al., 1985) showed that DHPC has a fast rate of axial diffusion at $T < 35°C$ in contrast to 1,2-dipalmitoylphosphatidylcholine (DPPC) at the same reduced temperature, suggesting that DHPC forms relatively disordered or less closely packed interdigitated bilayers.

The above-mentioned dynamic studies are confined to one component interdigitated systems. To mimic biological membranes, studies should be extended to include other membrane constituents. Interdigitated lipids mixed with fluorescent probes or spin labels serve as a good model system for studying interactions between interdigitated lipids and small molecules. Nambi et al. (1988) demonstrated that the ethanol-induced phase transition of DPPC and distearoylphosphatidylcholine (DSPC) from the noninterdigitated gel phase to the fully interdigitated phase can be monitored by analyzing the fluorescence intensity of 1,6-diphenyl-1,3,5-hexatriene (DPH). It was found that a significant decrease in DPH fluorescence intensity occurs during the phase transition. The decrease in intensity was interpreted to be the result of changes in the probe location from the center of the bilayer orientated parallel to the membrane surface to the disposition aligned parallel with the neighboring fatty acid chains (Nambi et al., 1988). This interpretation was supported by the data obtained with phosphatidylcholine-linked DPH which shows little change in fluorescence intensity through the same phase transition. Using spin labels, Boggs et al. (1989) showed that interdigitated gel phase bilayers have a much less steep fluidity gradient along the acyl chain, as compared with noninterdigitated gel phase bilayers. However, a detailed description in terms of rotational rate and hindrance of spin labels in interdigitated structures is not yet reported.

Recently, in our laboratory, differential scanning calorimetry (DSC) was employed to study the interactions of cholesterol with interdigitated lipids (Chong and Choate, 1989). Our DSC results suggest that cholesterol exhibits a disordering effect on the bilayer structure of mixed interdigitation. More recently, nanosecond fluorescence spectroscopy was employed to detect the rotation of dehydroergosterol (DHE), a fluorescent cholesterol analogue, in an interdigitated lipid membrane (Kao et al., 1990). The results further indicate that sterols have a disordering effect on the packing of mixed-interdigitated structures. In contrast, the presence of sterols results in an ordering effect on partially interdigitated bilayers. However, due to the lack of precise information of the orientation of the emission dipole moment of DHE, a detailed quantitative description of DHE rotation in the bilayer cannot be established. DPH, on the other hand, is well documented to be a fluorescent rod-shaped molecule (for a review, see Van Der Meer, 1988). Its emission dipole moment is known to be nearly colinear with the long axis of the probe molecule.

Therefore, it is advantageous to use DPH as a probe to explore the rotation of small molecules in interdigitated lipid membranes. In the present study, we studied 1-stearoyl-2-capryl-*sn*-glycero-3-phosphocholine [C(18):C(10)PC] which is an asymmetric mixed-chain phospholipid known to form highly ordered mixed-interdigitated structures below the transition temperature, T_m, and form relatively disordered, partially interdigitated bilayers above T_m (McIntosh et al., 1984; Hui et al., 1984; Mattai et al., 1987; Xu and Huang, 1987; Wong and Huang, 1989). We first employed a modified Y-plot method in terms of thermal coefficient of rotation to describe phenomenologically the rotation of DPH in C(18):C(10)PC bilayers, with the aid of DSC to relate rotation to the physical state of the matrix lipid. Then we used differential polarized phase-modulation fluorometry (Weber, 1978; Lakowicz et al., 1985) to obtain real-time data of DPH rotation in C(18):C(10)PC.

MATERIALS AND METHODS

Materials

DPH was purchased from Molecular Probes (Eugene, OR) and used as such. C(18):C(10)PC was synthesized by the method of Xu and Huang (1987). *p*-bis[2-(5-phenyloxazolyl)]benzene (POPOP) was purchased from Eastman Kodak Co. (Rochester, NY).

Liposome preparation

C(18):C(10)PC dissolved in chloroform was dried under vacuum overnight, and then suspended in 50 mM KCl and 0.02% NaN_3 at 37°C (which is above the T_m of C(18):C(10)PC) to form multilamellar vesicles (MLV). Then enough lipid was added to dried DPH in a test tube to form a DPH/lipid molar ratio of 1:500. The sample was subsequently put through three freeze-thaw cycles and then stored at least 48 h at 4°C before use.

Differential scanning calorimetric measurements

Calorimetric measurements were made with a Hart Scientific differential scanning calorimeter (Pleasant Grove, UT). The sample had been incubated at 4°C then loaded into the calorimeter cell at room temperature. The sample was brought down to 0°C and held for at least an hour at 0°C before the initial heating scan. The sample was subjected to two heating and cooling scans with the sample being held for 1 h between each scan. The data were corrected for machine hysteresis according to Kao et al. (1990). All DSC scans were made at a scan rate of 15°/h.

Fluorescence intensity and polarization measurements

Measurements of fluorescence polarization and emission intensity were made with an ISS Greg 200 fluorometer (ISS Inc., Champaign, IL) and

with an SLM 48000 spectrofluorometer (SLM Instruments Inc., Urbana, IL), respectively. The sample was excited at 325 nm. A dispersion of multilameller vesicles with a concentration of phosphate approximately equal to that in the sample was used as the blank solution for the polarization measurements to correct for scattered light. The polarization of the sample was measured through a cutoff filter (KV389; Schott Glass Technologies Inc., Duryea, PA). The standard deviation of the polarization values is approximately ± 0.004. The sample was constantly stirred using a magnetic bar during the intensity measurements.

Fluorescence lifetime measurements

Fluorescence lifetimes and anisotropy decays of DPH in C(18):C(10)PC were determined using the ISS Greg 200 fluorometer, an instrument based on the design of Gratton and Limkeman (1983). The light source was a He/Cd laser (model 4240B; Liconix Inc., Sunnyvale, CA). The excitation wavelength used was 325 nm. For lifetime measurements, the excitation polarizer was set at 35° with respect to the vertical plane and no emission polarizer was used. Phase and modulation values were determined relative to a POPOP (in ethanol) reference solution, which has a lifetime of 1.35 nm at 325 nm excitation. For anisotropy decay measurements, differential phase and demodulation ratio between parallel and perpendicular components were determined upon vertical excitation (Weber, 1978; Lakowicz et al., 1984). A Schott KV389 cutoff filter was used for DPH emission for both the intensity decay and the anisotropy decay measurements. Phase and modulation values were determined using modulation frequencies ranged from 5 to 100 MHz. The data were analyzed using the nonlinear least-squares program provided by ISS Inc. based on the scheme described in Jameson and Gratton (1983) and Lakowicz et al. (1984, 1985). Random errors of 0.4° for phase angle in lifetime measurements, 0.3° for phase angle in differential polarized phase measurements, and of 0.005 for modulation values were used in the least-squares fit. The cone angle (θ) and the wobbling diffusion coefficient (Dw) were calculated as described by Kinosita et al. (1977) using the values of σ estimated from their Fig. 3 *b*.

RESULTS

DSC measurements

Shown in Fig. 1 are the typical DSC heating and cooling thermograms for a C(18):C(10)PC dispersion containing DPH in the stoichiometric ratio of 1:500 DPH/lipid. The heating T_m is 18.8°C vs. that of 18.9°C for pure C(18):C(10)PC (18.6°C [Ali et al., 1989], 19.2°C [Xu and Huang, 1987]), and the cooling T_m is 13.3°C vs. 13.7°C for pure C(18):C(10)PC as determined by DSC. The onset temperature, T_o, and the completion temperature, T_c, are 18.0° and 19.9°C, respectively, for the heating scan, and the values of T_o and T_c are 14.3°C and 12.4°C, respectively, as determined by the cooling scan as shown in Fig. 1. For pure C(18):C(10)PC, heating T_o is 18.4°C and T_c is 19.4°C, cooling T_o is 14.7°C and T_c is 13.0°C. Moreover, the thermal hysteresis which exists in pure C(18):C(10)PC between the heating and cooling scans remains upon addition of DPH. These DSC results clearly indicate that DPH exerts no significant effect on the thermal behavior of C(18):C(10)PC bilayer at the DPH/lipid ratio of 1:500.

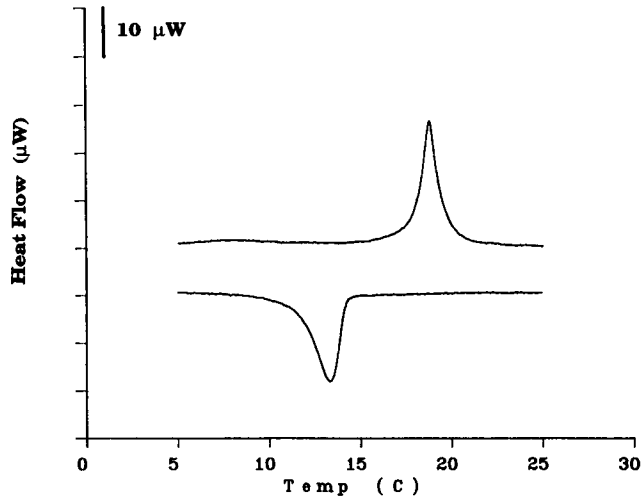

FIGURE 1 Typical heating and cooling DSC curves of DPH in C(18):C(10)PC (DPH/PC mole ratio is 1:500).

It should be noted that the lipid-to-probe ratio (500:1) is far below the critical value which alters the lipid properties (Lentz et al., 1976). Nambi et al. (1988) demonstrated that the ethanol-induced phase transition of DPPC and DSPC from the noninterdigitated gel phase to the fully interdigitated phase can be monitored by DPH fluorescence intensity using a lipid/probe ratio of 500:1, as confirmed by x-ray diffraction measurements. Our DSC data (Fig. 1) shows that the thermal parameters of DPH in C(18):C(10)PC are not significantly changed compared with those of pure C(18):C(10)PC. Thus, it can be assumed that C(18):C(10)PC maintains an interdigitated structure in the presence of DPH with the lipid/probe ratio of 500:1.

Thermal coefficient of rotation for DPH in C(18):C(10)PC

The thermal coefficient of the frictional resistance to the rotation of DPH in C(18):C(10)PC can be determined, in principle, by the method of Weber et al. (1984). However, this method does not take into account the limiting anisotropy which is not zero in membrane systems, and the discrepancy between the lipid diffusion and the classical hydrodynamic model (Vaz et al., 1984). Here, we present a method which covers the two points stated above. This method, designated as the modified Y-plot method, is described in detail in the Appendix. Using this method, we have determined the thermal coefficient of rotation of DPH in C(18):C(10)PC and compared the results with those obtained with a noninterdigitated lipid,

namely, 1,2-dimyristoyl-*sn*-glycerol-3-phosphocholine (DMPC).

Fig. 2 *A* shows the effect of increasing temperature on the steady-state fluorescence polarization of DPH in C(18):C(10)PC. DPH polarization decreases markedly in the temperature interval of 15–18°C on heating, and increases from 15–12°C on cooling (not shown). Thermal hysteresis is thus observed between the heating and cooling polarization values. The inset in Fig. 2 *A* shows the effect of increasing temperature on the total fluorescence intensity (from 350–550 nm) of DPH in C(18):C(10)PC. The fluorescence intensity (F) is seen to increase discontinuously from 13° to 18°C; it peaks at 19°C, thereafter the intensity decreases steadily with increasing temperature.

Fig. 2 *B* shows the lifetime measured at 20 MHz as a function of increasing temperature. The lifetime remains virtually unaltered until 16°C for heating and 14°C for cooling (not shown), where it drops, and then steadily decreases with increasing temperature.

Using Eq. A2, we obtained a membrane parameter, m, of 0.75 for C(18):C(10)PC. Using $r_0 = 0.39$ (Kawato et al., 1977), $m = 0.75$, the data shown in Fig. 2, and $T_R = 5.5$°C, Y_M can be calculated from Eq. A6. The dependence of Y_M on DPH in C(18):C(10)PC with heating and cooling scans is shown in Fig. 3, *A* and *B*, respectively.

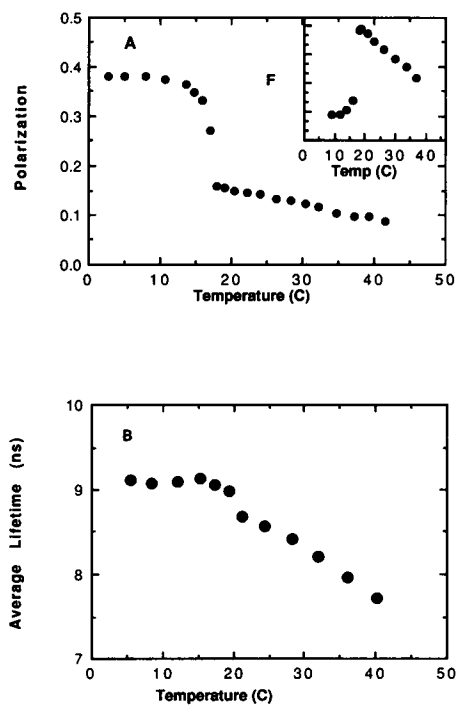

FIGURE 2 (*a*) Heating polarization of DPH in C(18):C(10)PC. (*Inset*) Effect of temperature on the fluorescence intensity of DPH. (*b*) Heating average lifetime of DPH in C(18):C(10)PC.

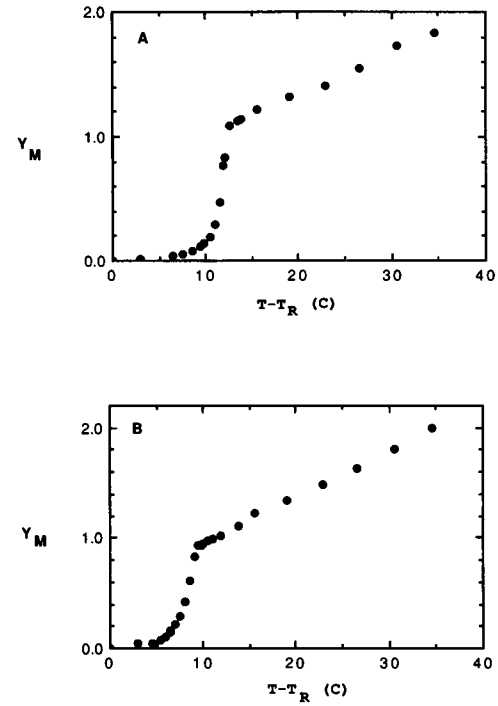

FIGURE 3 Modified Y-plot of DPH in C(18):C(10)PC as a function of temperature: (*a*) heating, and (*b*) cooling.

Thermal hysteresis is also obvious from the modified Y-plots.

For both the heating and cooling scans, all the data can be fitted with three lines. The slopes of the heating plot are: $b_{1M} = 0.004°C^{-1}$, $b_{2M} = 0.508°C^{-1}$, and $b_{3M} = 0.030°C^{-1}$. The breakpoint temperatures or critical temperatures (T_c) between these slopes are: $T_c(1) = 16.0$°C, and $T_c(2) = 18.1$°C. The slopes of the cooling plot are: $b_{1M} = 0.011°C^{-1}$, $b_{2M} = 0.408°C^{-1}$, and $b_{3M} = 0.042$ $°C^{-1}$. The cooling critical temperatures are: $T_c(1) = 12.7$°C, and $T_c(2) = 14.7$°C. The b_M values are summarized in Table 3, along with the b values determined by the Y-plot method of Weber et al. (1984). The b values determined by these two methods are somewhat different, but, the qualitative trend varying from b_1 to b_2 and to b_3 remains unchanged. The cooling critical temperatures obtained with the Y-plot shown in Fig. 3 *B* are significantly lower than those in the heating mode (Fig. 3 *A*). The scan rate for fluorescence measurement is estimated to be 2°/h. The DSC data also showed hysteresis (T_m[heating] = 18.9°C vs. T_m[cooling] = 13.3°C) (Fig. 1). The greater hysteresis observed in the DSC thermograms is due to the faster scan rate (15°/h). The hysteresis suggests that C(18):C(10)PC may freeze initially into a noninterdigitated bilayer. It may then become mixed interdigitated at a lower temperature. Similar observa-

tions and interpretation on the hysteresis for the ethanol-induced phase transition from the noninterdigitated to fully interdigitated DPPC have been made previously (Rowe, 1985; Boggs et al., 1989).

Fluorescence lifetime

Table 1 shows the resolved lifetimes of DPH in C(18):C(10)PC at different temperatures. The data were fit to the exponential decay law:

$$I(t) = \sum \alpha_i \exp(-t/\tau_i),$$

where $I(t)$ is the fluorescence intensity, α_i is the pre-exponential factor, and τ_i is the fluorescence lifetime from the ith component. $f_i = \alpha_i\tau_i/\Sigma\alpha_j\tau_j$, where f_i is the fraction of the total fluorescence intensity derived from the ith component. Among all the exponential decay laws tested, DPH emission in C(18):C(10)PC is best described by a double-exponential decay over the entire temperature range examined. The major component remains constant up to ~16°C, where it decreases thereafter. The average lifetime $\langle\tau\rangle = (\tau_1)f_1 + (\tau_2)f_2$ (Table 1) remains constant up to 17°C, where it drops and then steadily decreases with increasing temperature.

Analysis of the lifetime using Lorentzian distribution (Alcala et al., 1987) (Table 2), shows that the width of the major lifetime component remains 0.13–0.15 ns at temperatures below the onset temperature. Above the onset temperature, the width of the major lifetime component becomes narrower (0.05–0.10 ns).

Anisotropy decay measurement

The data of the differential phase and demodulation ratio were fitted by the equation: $r(t) = r_1e^{-t/\theta 1} + r_2e^{-t/\theta 2}$. In fitting the data, we fixed $\theta_1 = 10{,}000$ ns, and let r_1 become the floating parameter. In this case r_1 is essentially the limiting anisotropy r_∞. It is judged from the reduced χ^2 that, among other models tested, the equation: $r(t) = r_\infty + r_2e^{-t/\theta 2}$ best fits the data. Table 1 lists the fitted limiting anisotropy and rotational correlation times, θ_2, for DPH in C(18):C(10)PC as a function of increasing temperature. Fig. 4 *A* shows the effect of increasing temperature on the rotational correlation time of DPH in C(18):C(10)PC. The data are seen to steadily decrease with increasing temperature. Fig. 4 *B* shows the limiting anisotropy of DPH in C(18):C(10)PC as a function of temperature. The order parameter, S, as a function of temperature is shown in the inset. S is calculated according to the equation: $r_\infty/r_0 = S^2$. Both r_∞ and S show a dramatic decrease at ~16°C. Fig. 5 *A* shows the cone angle (θ) of DPH in C(18):C(10)PC as a function of increasing temperature. The cone angle steadily increases up to ~16°C where it undergoes an abrupt increase and then slowly increases again. Fig. 5 *B* show the wobbling diffusion constant (Dw) of DPH in C(18):C(10)PC as a

TABLE 2 Lorentzian distribution fit of DPH in C(18):C(10)PC

Temp	τ_1	w_1	f_1	τ_2	w_2	χ^2
C	*ns*			*ns*		
5.5	9.69	0.14	0.91	2.93	0.76	4.46
8.5	9.52	0.15	0.94	2.10	1.18	5.21
12.0	9.49	0.13	0.95	1.80	0.05	6.10
15.3	9.75	0.07	0.92	2.33	0.05	7.03
17.4	9.64	0.06	0.93	2.36	0.05	4.37
21.1	9.11	0.05	0.95	1.75	0.41	11.85
24.5	8.98	0.05	0.94	1.90	0.82	7.30
28.3	8.84	0.05	0.94	1.91	0.83	7.75
32.0	8.60	0.10	0.95	1.44	0.05	6.02
36.0	8.37	0.09	0.94	1.57	0.05	4.94
40.1	8.19	0.08	0.93	1.53	0.05	4.93

TABLE 1 DPH in C(18):C(10)PC lifetime and rotational data

Temp	τ_1	f_1	α_1	τ_2	χ^2	$\langle\tau\rangle$	r_∞	θ_2	r_2	χ^2
°C	*ns*			*ns*		*ns*		*ns*		
5.5	9.61 ± 0.15	0.93	0.77	2.39 ± 0.32	1.87	9.11	0.28 ± 0.01	4.03 ± 3.28	0.01 ± 0.00	1.23
8.5	9.49 ± 0.12	0.95	0.77	1.76 ± 0.26	2.22	9.07	0.26 ± 0.01	5.57 ± 1.83	0.03 ± 0.00	1.05
12.0	9.53 ± 0.14	0.95	0.77	1.84 ± 0.32	2.71	9.15	0.23 ± 0.00	2.48 ± 0.71	0.03 ± 0.00	1.72
15.3	9.77 ± 0.16	0.92	0.73	2.35 ± 0.28	3.04	9.18	0.19 ± 0.01	3.93 ± 0.61	0.07 ± 0.00	3.02
17.4	9.56 ± 0.12	0.94	0.76	2.17 ± 0.26	1.73	9.12	0.04 ± 0.00	3.47 ± 0.19	0.21 ± 0.00	3.58
19.3	9.37 ± 0.12	0.95	0.78	1.82 ± 0.33	3.28	8.98	0.04 ± 0.00	3.00 ± 0.11	0.23 ± 0.00	2.05
21.1	9.00 ± 0.12	0.96	0.78	1.44 ± 0.35	3.56	8.68	0.03 ± 0.00	3.25 ± 0.13	0.22 ± 0.00	2.01
24.5	8.94 ± 0.11	0.95	0.77	1.65 ± 0.30	3.01	8.56	0.03 ± 0.00	2.58 ± 0.09	0.24 ± 0.00	1.26
28.3	8.81 ± 0.12	0.94	0.77	1.73 ± 0.29	3.10	8.41	0.02 ± 0.00	2.34 ± 0.07	0.24 ± 0.00	1.38
32.0	8.57 ± 0.09	0.95	0.75	1.43 ± 0.25	2.62	8.20	0.02 ± 0.00	1.97 ± 0.08	0.24 ± 0.00	1.86
36.0	8.41 ± 0.10	0.93	0.74	1.64 ± 0.22	2.24	7.96	0.01 ± 0.00	1.46 ± 0.06	0.26 ± 0.01	1.82
40.1	8.18 ± 0.10	0.93	0.71	1.53 ± 0.20	2.25	7.72	0.01 ± 0.00	1.54 ± 0.08	0.23 ± 0.01	2.07

θ_1 is 10,000 ns.

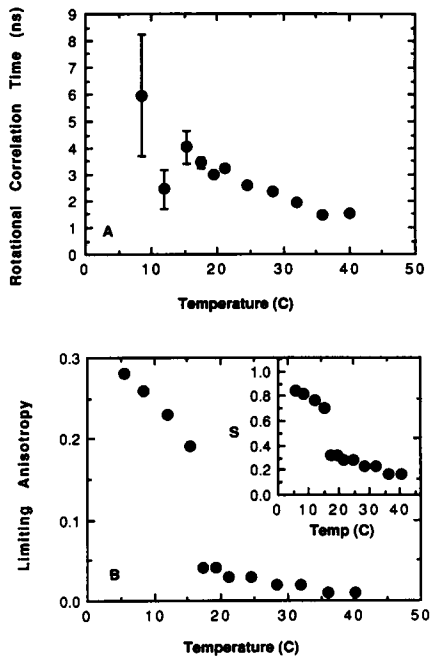

FIGURE 4 (*a*) Rotational correlation time of DPH in C(18):C(10)PC as a function of increasing temperature. (*b*) Limiting anisotropy of DPH in C(18):C(10)PC as a function of increasing temperature. (*Inset*) Order parameter, *S*, of the lipid as a function of increasing temperature.

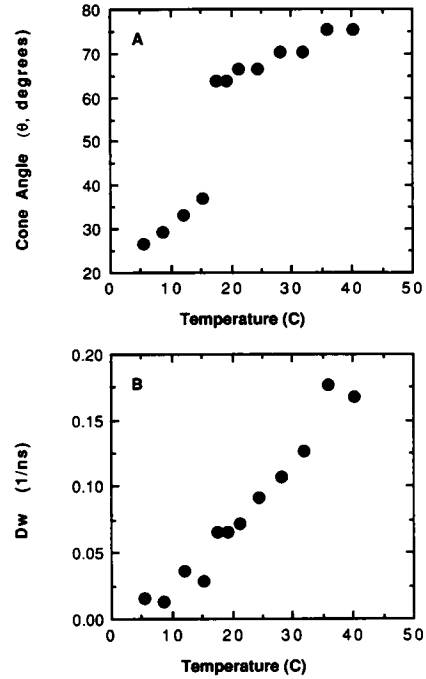

FIGURE 5 Effect of increasing temperature upon: (*a*) cone angle (θ), and (*b*) wobbling diffusion constant (*Dw*) of DPH in C(18):C(10)PC. Values were calculated according to the method of Kinosita et al. (1977).

function of increasing temperature. The *Dw* is seen to steadily increase with increasing temperature.

DISCUSSION

Previous DSC (Mason et al., 1981; Xu and Huang, 1987) and Raman (Huang et al., 1983) data showed that the mixed-interdigitated structures are highly ordered, even more ordered than the gel state of the corresponding noninterdigitated symmetric diacylphosphatidylcholines of the same molecular weight (e.g., C(18):C(10)PC vs. DMPC). At 10°C below T_m the values of Raman peak height intensity ratio $I(2{,}935\ cm^{-1})/I(2{,}884\ cm^{-1})$ obtained for C(18):C(10)PC and DMPC dispersions are 0.39 and 0.45, respectively (Huang et al., 1982, 1983), indicating that the interchain order of mixed-interdigitated C(18):C(10)PC is greater than that of DMPC in the gel state. In addition, the entropy change ΔS of the phase transition for C(18):C(10)PC is much greater than that for DMPC (30.3 eu/mol vs. 18.2 eu/mol) (Mason et al., 1981; Xu and Huang, 1987), also suggesting that mixed-interdigitated C(18):C(10)PC has a more ordered lipid packing than DMPC in the gel state. It is therefore rather surprising that DPH retains considerable rotational mobility in highly ordered mixed interdigitated C(18):C(10)PC lipid membranes. The b_{2M} values obtained for DPH in C(18):C(10)PC are comparable to those obtained for DPH in noninterdigitated phosphatidylcholine bilayers (e.g., DMPC) (Table 3). This indicates that the change in rotational diffusion per degree in the phase transition between mixed-interdigitated and partially interdigitated bilayers is not much higher than that between noninterdigitated phases. The r_∞ values in the mixed-interdigitated state (Fig. 4) are not higher than those in the gel state of noninterdigitated lipid bilayers (e.g., $r_\infty \approx 0.33$ in DMPC; Lakowicz et al., 1979), which indicates that the acyl chain order derived from DPH fluorescence is about the same between a mixed-interdigitated structure and a noninterdigitated gel state. The discrepancy between DPH data and previous Raman data (Huang et al., 1983) can be reconciled as follows.

The DPH rotation reflects that the fluorophore is experiencing some motional order in the intermolecular spacing (referring to the immediate surrounding near DPH) between the C(18):C(10)PC interdigitated acyl chains, whereas the Raman data (Huang et al., 1983) based on the C–H stretching in the methylene units reports the chain–chain interactions and the intermolecular ordering in the absence of membrane perturbants. The acyl chains of the mixed-interdigitated C(18):C(10)PC are highly ordered, even more ordered than those of the

TABLE 3 **Thermal coefficient *b* in interdigitated lipid bilayers vs. noninterdigitated bilayers***

Sample		b_1	b_{1M}	$b_2^{\ddagger}$	$b_{2M}^{\ddagger}$	b_3	b_{3M}	
DPH/C(18):C(10)PC	heating	0.007	0.004	0.773	0.508	0.027	0.030	this work
	cooling	0.038	0.011	0.667	0.408	0.043	0.042	this work
DPH/DMPC		0.003	0.000	0.682	0.464	0.056	0.054	this work
DPH/DMPC		0.078		0.307		0.056		derived from Parasassi et al. (1984)
11-AU/DMPC§		0.036		0.118		0.065		derived from Scarlata (1989)
DPH/DPPC		0.017		0.449		0.046		derived from Parasassi et al. (1984)
DPH/DLPE		0.040		0.250		0.050		Chong and Thompson (1986)

*b values are in $°C^{-1}$. All vesicles are MLV. b_1, b_2, and b_3 are the thermal coefficients calculated based on the original Y-plot method of Weber et al. (1984). b_{1M}, b_{2M}, and b_{3M} are the thermal coefficients derived from the modified Y-plot method described in the Appendix.
‡Refers to the b values during the gel-to-liquid crystalline phase transition.
§11-AU is 11-(9)-anthroyloxy-undecanoic acid.

noninterdigitated diacylphosphatidylcholines in the gel state; but, the restriction on the rotation of DPH within the intermolecular spacing where the fluorophores are accomodated bears little difference between the mixed-interdigitated and the noninterdigitated gel state. This result can be understood in terms of the steric hindrance imposed by the bulky terminal methyl group in the hydrocarbon chain. Two situations are considered here. The situation I shown in Fig. 6 suggests that DPH may slip into a pocket area somewhere between the two terminal methyl groups along the long acyl chains of the neighboring C(18):C(10)PC molecules. The advantage of this arrangement is that DPH avoids the steric hindrance due to the bulky terminal methyl groups. However, it would create void volume at both ends of the probe which is energetically unfavorable. Note that the effective volume of the terminal methyl group is about twice that of a methylene unit in the hydrocarbon chain (Reiss-Husson and Luzzati, 1964; Flory, 1969). Because the intermolecular order of mixed-interdigitated C(18):C(10)PC is known to be higher than that of noninterdigitated gel state (e.g., DMPC gel state) (Huang et al., 1983), DPH in situation I should, in principle, possess a more ordered rotation, hence a higher r_∞ value. Our data (Fig. 4), however, showed that this is not the case. Alternatively, DPH may insert itself into mixed-interdigitated C(18):C(10)PC as depicted in situation II of Fig. 6. In this case, two DPH molecules (~13 Å long for each; Shinitzky and Barenholz, 1974) are aligned between two mixed-interdigitated units (a bilayer thickness of ~33 Å). The advantage of this arrangement is to maximize the van der Waal's interactions. As such, each DPH molecule has direct contact with one terminal methyl group. Due to the steric hindrance imposed by terminal methyl groups, the intermolecular spacing where DPH is accommodated becomes larger than what is expected for the mixed-interdigitated structure of pure C(18):C(10)PC. This enlarged spacing compensates for the overall ordered structure due to mixed interdigitation in such a way that all dynamic parameters of DPH rotation bear little difference between the mixed-interdigitated and the non-interdigitated gel state. To our knowledge, this is the first time that the contribution of the bulky terminal methyl groups is considered when interpreting the data derived from fluorescent probes in lipid bilayers. In any event, our DPH result may be of great biological importance because it implies that considerable rotational mobility of self-inserted small molecules (e.g., a peptide segment or a steroid molecule) can be sustained in an intramolecularly highly order interdigitated lipid matrix. In fact, Kao et al. (1990) recently also showed that the rotation of dehydroergosterol is appreciable in mixed-interdigitated C(18):C(10)PC structures.

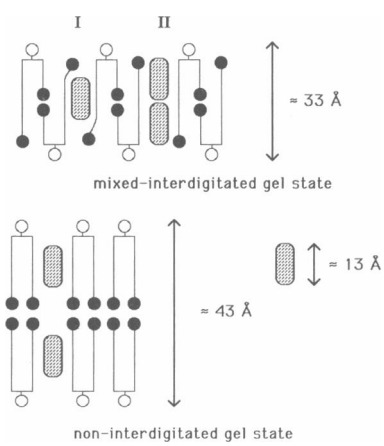

FIGURE 6 Schematic diagram showing the steric interactions between the terminal methyl groups and DPH. The dark circles represent the bulky terminal methyl groups.

The b_{2M}, r_∞, and θ_2 values of DPH in C(18):C(10)PC undergo an abrupt change near the onset temperature of the phase transition as determined by DSC. Thus, we demonstrate here that certain fluorescence parameters of DPH other than emission intensity are sensitive to transi-

tions between mixed interdigitated and partially interdigitated phases. Nambi et al. (1988) observed that the fluorescence intensity of DPH is decreased during the ethanol-induced phase transition from noninterdigitated to fully interdigitated phases. The decrease in intensity was attributed to the probe relocation from a disposition perpendicular to the acyl chain of the PC in the center of the bilayer (Ameloot et al., 1984; Davenport et al., 1985) to either a disposition parallel to the acyl chain and aligned side by side to the neighboring PC or to a location in the lipid–water interface (Nambi et al., 1988). The mixed-interdigitated C(18):C(10)PC cannot accommodate DPH in the center of the bilayer due to the overlapping chains; but, the relatively disordered, partially interdigitated C(18):C(10)PC may accommodate DPH in the center of the bilayer. Therefore, a decrease in DPH fluorescence intensity from the disordered to ordered state of C(18):C(10)PC is expected, which is exactly the case observed (Fig. 2 *A*, *insert*). Combining our intensity results with those obtained by Nambi et al. (1988), it seems appropriate to use probe relocation to explain the DPH intensity change observed by Nambi et al. (1988) because the rationale used by Nambi et al. (1988) predicts correctly the situation in C(18):C(10)PC shown in this study.

The emission of DPH in C(18):C(10)PC has been analyzed by both a multi-exponential decay law and continuous distribution functions. It is found that the fluorescence emission of DPH in C(18):C(10)PC is best described by either a double-exponential decay or a Lorentzian distribution (Tables 1 and 2). These results are qualitatively in good agreement with those obtained with DPH in DMPC and in DPPC (Fiorini et al., 1987), and in POPC (Williams and Stubbs, 1988). The noticeable, but interesting, differences between these studies lie in the full width at half maximum of the Lorentzian distribution of the major lifetime component (w_1 in Table 2). Fiorini et al. (1987) reported that, below T_m, w_1 was ~0.6 ns. w_1 dropped to ~0.1 ns at T_m and above T_m. Their interpretation was that the lifetime distribution originates from a continuum of different environments of the DPH molecules due to different dielectric constants along the acyl chain. Below T_m, the dielectric constant gradient along the acyl chain determines the distribution of decay rates. Above T_m, the lipid packing becomes loose; thus, the translational and rotational mobility of DPH increases, which makes the DPH experience an average environment during fluorescence lifetime. This explains the drop of w_1 from 0.6 to 0.1 ns through the gel-to-liquid crystalline phase transition of DPPC and DMPC (Fiorini et al., 1987). However, our data in Table 2 shows that the change in w_1 from the mixed-interdigitated to the partially interdigitated state is much less. w_1 is 0.13–0.15 ns in the mixed-interdigitated state ($\leq$12°C; Table 2). Above the onset temperature (16°C), the w_1 drops slightly to 0.05–0.10 ns. The values of w_1 in the partially interdigitated C(18):C(10)PC (0.05–0.10 ns) are comparable to those of DPPC, DMPC, and POPC in the liquid-crystalline state (~0.1 ns) (Fiorini et al., 1987; Williams and Stubbs, 1988). However, the values of w_1 in the mixed-interdigitated C(18):C(10)PC (0.13–0.15 ns) are significantly lower than those of DPH for DPPC and DMPC in the gel state (w_1 = 0.6 ns; Fiorini et al., 1987). This difference can be explained by the concept of dielectric constant gradient (Fiorini et al., 1987). The dielectric constant gradient along the acyl chain of mixed-interdigitated C(18):C(10)PC is probably much less steep than that of noninterdigitated bilayers of the same molecular weight due to the significant difference in bilayer thickness. The bilayer thickness of mixed-interdigitated C(18):C(10)PC is reported to be 33–34 Å (Hui et al., 1984; McIntosh et al., 1984) which is 10 Å shorter than the bilayer thickness of DMPC in the gel state. It is of interest to note that Boggs et al. (1989) used spin labels to show that interdigitated gel phase bilayers have a much less steep fluidity gradient along the acyl chain. Thus, our data presented here echo the idea that the continuous distribution of DPH lifetime in the gel state of a single component PC liposome is due to the heterogeneity of the environment of DPH along the acyl chain (Fiorini et al., 1987; Williams and Stubbs, 1988).

In conclusion, in this study, we have characterized the dynamic behavior of DPH in interdigitated C(18):C(10)PC bilayers. We have demonstrated that fluorescence dynamic parameters of DPH as well as its intensity can be used to monitor the liquid-crystalline-to-gel phase transition between partially and mixed-interdigitated C(18):C(10)PC. Through the unique structure of mixed-interdigitated C(18):C(10)PC, our results echo two assertions made previously by other investigators. Our data support the idea that DPH relocation occurs during the phase transition of extensive lipid interdigitation (Nambi et al., 1988). Our data also echo the idea that the width of DPH lifetime distribution (major component) in the gel state of PC bilayers is related to heterogeneity in dielectric constant along the acyl chain of lipids (Fiorini et al., 1987). More importantly, our present results, combined with those obtained with cholesterol and DHE in C(18):C(10)PC (Chong and Choate, 1989; Kao et al., 1990), suggest that, once inserted into the interdigitated lipid matrix, membrane perturbants are able to create disordered local environments for rotational mobility no matter whether the lipid matrix is extensively interdigitated. The membrane perturbants could be sterols, probes such as DPH, or membrane-bound proteins or peptides. This may explain how a vital membrane component retains its physiological function in interdigitated lipid environments if such environments exist in biological mem-

branes. A study on the interactions of cytochrome b5 with interdigitated C(18):C(10)PC bilayers is currently being undertaken in our laboratory to substantiate this hypothesis.

APPENDIX

A modified Y-plot method

by B. Wieb Van Der Meer

Weber and co-workers introduced the Y-plot method for the fluorescence anisotropy of fluorophores in isotropic solvents and proteins (Weber et al., 1984). Here we will generalize this method to the case of lipid-like fluorescent probes in membranes. The steady-state fluorescence anisotropy from fluorophores in membranes is related to the wobbling diffusion constant, D_W, the average lifetime, $\langle\tau\rangle$, and the "membrane parameter," m, through an extended Perrin equation (Van Der Meer et al., 1986):

$$r_0/r - 1 + m = 6D_W\langle\tau\rangle. \quad \text{(A1)}$$

The membrane parameter, m, can be obtained by fitting (r_∞, r)-data to:

$$r_\infty/r_0 = (r/r_0)^2/\{r/r_0 + (1 - r/r_0)^2/m\}. \quad \text{(A2)}$$

This equation has been derived by Van Der Meer et al. (1986). Fitting (r_∞, r)-data to Eq. A2 for the C(18):C(10)PC system studied in the present paper yields $m = 0.75$ (see Fig. 7). In isotropic solvents and proteins, the rotational diffusion constant may be related to the viscosity of the solvent by applying the hydrodynamic model (Weber et al., 1984). However, lateral diffusion data in membranes indicate that the hydrodynamic model does not apply to lipid diffusion, at least not to lateral diffusion of lipids (Vaz et al., 1984). Therefore, we will not attempt to relate D_W to a viscosity that decreases exponentially with temperature as in the original Y-plot method. Instead, we will assume that D_W itself increases exponentially with temperature according to:

$$D_W = D_{WR} \exp[b(T - T_R)]. \quad \text{(A3)}$$

where T_R is an arbitrarily chosen reference temperature, D_{WR} is the wobbling diffusion constant of the probe at T_R, and b_M is a parameter which we will call the "thermal coefficient for wobbling diffusion."

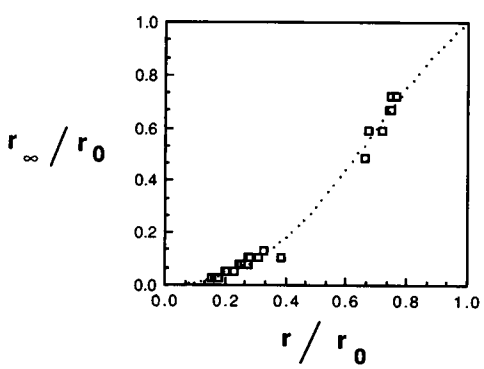

FIGURE 7 Data of r_∞/r_0 and r/r_0 for DPH with $r_0 = 0.39$ in C(18):C(10)PC at temperatures between 5.5 and 40.1°C and the best fit (*dotted line*) to Eq. A2 corresponding to $m = 0.75$.

Substituting Eq. A3 into Eq. A1 gives:

$$r_o/r - 1 + m = 6D_{WR}\langle\tau\rangle_R\{\langle\tau\rangle/\langle\tau\rangle_R\}\exp[b_M(T - T_R)], \quad \text{(A4)}$$

where $\langle\tau\rangle_R$ is the average lifetime at T_R. Using Eq. A1 at T_R, where the steady-state anisotropy equals r_R:

$$r_o/r_R - 1 + m = 6D_{WR}\langle\tau\rangle_R \quad \text{(A5)}$$

to eliminate $6D_{WR}\langle\tau\rangle_R$ and taking the natural logarithm we can now introduce Y_M (the modified Y) as follows:

$$Y_M = \mathrm{LN}\{[r_0r_R\langle\tau\rangle_R + (m - 1)rr_R\langle\tau\rangle_R]/[r_0r\langle\tau\rangle + (m - 1)rr_R\langle\tau\rangle]\}$$
$$= b_M(T - T_R). \quad \text{(A6)}$$

Thus, a plot of Y_M vs. $t = T - T_R$ should yield a straight line if b_M is independent of temperature.

We thank Professor Fu-Ming Chen for using the SLM 48000 fluorometer.

This work was supported in part by a grant from the National Science Foundation (NSF-MRCE, grant no. R11-8714805 to Meharry Medical College) and a grant from the U.S. Army Research Office (to Dr. Chong), and in part by a grant from the National Institutes of Health (GM 17452 to Dr. Huang). This work was done during the tenure of an Established Investigatorship (to Dr. Chong) from the American Heart Association and CIBA GEIGY. Ms. Kao is a recipient of the Department of Education Patricia-Roberts-Harris Fellowship.

Received for publication 30 April 1990 and in final form 21 June 1990.

REFERENCES

Alcala, J. R., E. Gratton, and F. G. Prendergast. 1987. Resolvability of fluorescence lifetime distributions using phase fluorometry. *Biophys. J.* 51:587–596.

Ali, S., H. Lin, R. Bittman, and C. Huang. 1989. Binary mixtures of saturated and unsaturated mixed-chain phosphatidylcholines. A differential scanning calorimetry study. *Biochemistry.* 28:522–528.

Ameloot, M., H. Hendrickx, W. Herreman, H. Pottel, R. Van Cauwelaert, and B. W. Van Der Meer. 1984. Effect of orientational order on the decay of the fluorescence anisotropy in membrane suspensions. Experimental verification on unilamellar vesicles and lipid/α-lactalbumin complexes. *Biophys. J.* 46:525–539.

Boggs, J. M., G. Rangaraj, and A. Watts. 1989. Behavior of spin label in a variety of interdigitated lipid bilayers. *Biochim. Biophys. Acta.* 981:243–253.

Chong, P. L.-G., and D. Choate. 1989. Calorimetric studies of the effects of cholesterol on the phase transition of C(18):C(10)phosphatidylcholine. *Biophys. J.* 55:551–556.

Chong, P. L.-G., and T. E. Thompson. 1986. Depolarization of dehydroergosterol in phospholipid bilayers. *Biochim. Biophys. Acta.* 863:53–62.

Davenport, L., R. E. Dale, R. H. Bisby, and R. B. Cundall. 1985. Transverse location of the fluorescent probe 1,6-diphenyl-1,3,5-hexatriene in model lipid bilayer membrane systems by resonance excitation energy transfer. *Biochemistry.* 24:4097–4108.

Fiorini, R. M., M. Valentino, S. Wong, M. Glaser, and E. Gratton.

1987. Fluorescence lifetime distributions of 1,6-diphenyl-1,3,5-hexatriene in phospholipid vesicles. *Biochemistry*. 26:3864–3870.

Flory, P. J. 1969. Statistical Mechanics of Chain Molecules. Wiley Interscience, New York.

Gratton, E., and M. Limkeman. 1983. A continuously variable frequency cross-correlation phase fluorometer with picosecond resolution. *Biophys. J.* 44:315–324.

Huang, C., and J. T. Mason. 1986. Structure and properties of mixed-chain phospholipid assemblies. *Biochim. Biophys. Acta.* 864: 423–470.

Huang, C., J. R. Lapiedes, and I. W. Levin. 1982. Phase transition behavior of saturated, symmetric chain phospholipid bilayer dispersions determined by Raman spectroscopy: correlation between spectral and thermodynamic parameters. *J. Am. Chem. Soc.* 104:5926–5930.

Huang, C., J. T. Mason, and I. W. Levin. 1983. Raman spectroscopic study of saturated mixed-chain phosphatidylcholine multilamellar dispersions. *Biochemistry*. 22:2775–2780.

Hui, S. W., J. T. Mason, and C. Huang. 1984. Acyl chain interdigitation in saturated mixed-chain phosphatidylcholine bilayer dispersions. *Biochemistry*. 23:5570–5577.

Jameson, D. M., and E. Gratton. 1983. Analysis of the heterogeneous emission by multifrequency phase and modulation fluorometry. *In* New Direction in Molecular Luminesce. D. Eastwood, editor. Am. Soc. Test. and Mater., ASTM Special Technical Publication. 822:67–81.

Kao, Y. L., P. L.-G. Chong, and C. Huang. 1990. Time-resolved fluorometric and differential scanning calorimetric investigation of dehydroergosterol in 1-stearoyl-2-caprylphosphatidylcholine bilayers. *Biochemistry*. 29:1315–1322.

Kawato, S., K. Kinosita, Jr., and A. Ikegami. 1977. Dynamic structure of lipid bilayers studied by nanosecond fluorescence technique. *Biochemistry*. 16:2319–2324.

Kinosita, K., Jr., S. Kawato, and A. Ikegami. 1977. A theory of fluorescence polarization decay in membranes. *Biophys. J.* 20:289–305.

Lakowicz, J. R., F. G. Prendergast, and D. Hogen. 1979. Fluorescence anisotropy measurements under oxygen quenching conditions as a method to quantify the depolarizing rotations of fluorophores. *Biochemistry*. 18:520–527.

Lakowicz, J. R., H. Cherek, B. P. Maliwal, E. Gratton, and M. Limkeman. 1984. Analysis of fluorescence decay kinetics from variable-frequency phase shift and modulation data. *Biophys. J.* 46:463–477.

Lakowicz, J. R., H. Cherek, B. P. Maliwal, and E. Gratton. 1985. Time-resolved fluorescence anisotropies of diphenylhexatriene and perylene in solvents and lipid bilayers obtained from multifrequency phase-modulation fluorometry. *Biochemistry*. 24:376–383.

Lentz, B. R., Y. Barenholz, and T. E. Thompson. 1976. Fluorescence depolarization studies of phase transitions and fluidity in phospholipid bilayers. 1. Single component phosphatidylcholine liposomes. *Biochemistry*. 15:4521–4528.

Mason, J. T., C. Huang, and R. L. Biltonen. 1981. Calorimetric investigations of saturated mixed-chain phosphatidylcholine bilayer dispersions. *Biochemistry*. 20:6086–6092.

Mattai, J., P. K. Sripada, and G. G. Shipley. 1987. Mixed-chain phosphatidylcholine bilayers: structure and properties. *Biochemistry*. 26:3287–3297.

McIntosh, T. J., S. A. Simon, J. C. Ellington, and N. A. Porter. 1984. New structural model for mixed-chain phosphatidylcholine bilayers. *Biochemistry*. 23:4038–4044.

Nambi, P., E. S. Rowe, and T. J. McIntosh. 1988. Studies of the ethanol-induced interdigitated gel phase in phosphatidylcholines using the fluorophore 1,6-diphenyl-1,3,5-hexatriene. *Biochemistry*. 27:9175–9182.

Parasassi, T., F. Conti, M. Glaser, and E. Gratton. 1984. Detection of phospholipid phase separation. *J. Biol. Chem.* 259:14011–14017.

Reiss-Husson, F., and V. Luzzati. 1964. The structure of the micellar solutions of some amphiphilic compounds in pure water as determined by absolute small-angle x-ray scattering techniques. *J. Phys. Chem.* 68:3504–3511.

Rowe, E. S. 1985. Thermodynamic reversibility of phase transitions. Specific effects of alcohols on phosphatidylcholines. *Biochim. Biophys. Acta.* 813:322–330.

Ruocco, M. J., D. J. Simonovitch, and R. G. Griffin. 1985. Comparative study of the gel phase of ether- and ester-linked phosphatidylcholines. *Biochemistry*. 24:2406–2411.

Scarlata, S. F. 1989. Evaluation of the thermal coefficient of the resistance to fluorophore rotation in model membranes. *Biophys. J.* 55:1215–1223.

Shinitzky, M., and Y. Barenholz. 1974. Dynamics of the hydrocarbon layer in liposomes of lecithin and sphingomyelin containing dicetylphosphate. *J. Biol. Chem.* 249:2652–2657.

Siminovitch, D. J., K. R. Jeffrey, and H. Eibl. 1983. A comparison of the headgroup conformation and dynamics in synthetic analogs of DPPC. *Biochim. Biophys. Acta.* 727:122–134.

Singer, S. J., and G. L. Nicolson. 1972. The fluid mosaic model of the structure of cell membranes. *Science (Wash. DC).* 175:720–731.

Slater, J. L., and C. Huang. 1988. Interdigitated bilayer membranes. *Prog. Lipid Res.* 27:325–359.

Van Der Meer, B. W. 1988. Biomembrane structure and dynamics viewed by fluorescence. *In* Subcellular Biochemistry. Hilderson, H. J., editor. Plenum Press, New York. 13:1–53.

Van Der Meer, B. W., R. P. van Hoeven, and W. J. van Blitterswijk. 1986. Steady-state fluorescence polarization data in membranes. Resolution into physical parameters by an extended Perrin equation for restricted rotation of fluorophores. *Biochim. Biophys. Acta.* 854:38–44.

Vaz, W. L. C., F. Goodsaid-Zalduondo, and K. Jacobson. 1984. Lateral diffusion of lipids and proteins in bi-layer membranes. *FEBS (Fed. Eur. Biochem. Soc.) Lett.* 174:199–208.

Weber, G. 1978. Limited rotational motion: recognition by differential phase fluorometry. *Acta. Phys. Pol.* A54:859–865.

Weber, G., S. Scarlata, and M. Rholam. 1984. Thermal coefficient of the frictional resistance to rotation in simple fluorophores determined by fluorescence polarization. *Biochemistry*. 23:6785–6788.

Williams, B. W., and C. Stubbs. 1988. Properties influencing fluorophore lifetime distributions in lipid bilayers. *Biochemistry*. 27:7994–7999.

Wong, P. T. T., and C. Huang. 1989. Structural aspects of pressure effects on infrared spectra of mixed-chain phosphatidylcholine assemblies in D_2O. *Biochemistry*. 28:1259–1263.

Xu, H., and C. Huang. 1987. Scanning calorimetry study of fully hydrated asymmetric phosphatidylcholines with one acyl chain twice as long as the other. *Biochemistry*. 26:1036–1043.